

# Synthesis of superheavy elements beyond $Z=118$

M. Mirea<sup>1</sup>, D.S. Delion<sup>1,2</sup> and A. Săndulescu<sup>2,3</sup>

<sup>1</sup>*National Institute of Physics and Nuclear Engineering,  
407 Atomistilor, Bucharest-Măgurele, Romania*

<sup>2</sup>*Academy of Romanian Scientists  
Splaiul Independenței 54, Bucharest, Romania*

<sup>3</sup>*Institute for Advanced Studies in Physics,  
Calea Victoriei 129, Bucharest, Romania*

We investigate the cold fission/fusion paths of superheavy nuclei within the two center shell model, in order to find the best projectile-target combinations of their production. The fission/fusion yields are estimated by using the semiclassical approach. We predict several asymmetric combinations of relative long living fragments, which can be used in fusion experiments of superheavy nuclei with  $Z > 118$ .

PACS numbers: 21.10.Dr, 21.10.Tg, 25.70.Jj, 25.85.Ca

Keywords: Cold fission, Superheavy nuclei, Potential surface, Cold valleys, Two center shell model, Woods-Saxon potential

The synthesis of superheavy elements beyond  $Z = 104$ , suggested by Flerov [1], was predicted within the so-called fragmentation theory in Ref. [2] by using the cold valleys in the potential energy surface between different combinations, giving the same compound nucleus. Soon it was shown in Refs. [3, 4] that the most favorable combinations with  $Z \geq 104$  are connected with the so-called Pb potential valley, i.e. the same valley of the heavy cluster emission [5].

Due to the double magicity of  $^{48}\text{Ca}$ , similar with  $^{208}\text{Pb}$ , in Ref. [4] it was proposed  $^{48}\text{Ca}$  as a projectile on various transuranium targets. Indeed, the production of many superheavy elements with  $Z \leq 118$  (corresponding to the last stable element Cf) during last three decades was mainly based on this idea [6, 7, 8, 9].

The formation of superheavy compound systems by fusion was intensively explored [10, 11, 12]. On the other side the investigation of experimental data concerning fusion and fission of superheavy nuclei with  $Z = 112, 114, 116$ , together with data on survival probability of these nuclei in evaporation channels with 3-4 neutrons, revealed the fact that the fission barriers are quite high, leading to a relative high stability of such systems [13].

The main tool to investigate such nuclei is almost exclusively based upon the investigation of  $\alpha$ -decay chains. In the last decade several papers were devoted to the calculation of  $\alpha$ -decay half-lives in this region [14]. All these approaches can be considered as phenomenological ones, based essentially on the Gamow  $\alpha$ -nucleus potential picture [15]. The recent microscopic estimate of the  $\alpha$ -particle preformation factor, by using shell model single particle orbitals, performed in Ref. [16], showed that the strong change of the  $Q$ -value along neutron chains can be explained only by supposing the existence of an  $\alpha$ -cluster component in heavy and superheavy emitters.

The  $\alpha$ -particle emission is connected with the "lightest" side of the cold valley on the fragmentation potential surface. On the other hand the "heaviest" side of the cold valley is given by the cold fission process, i.e. the emission of two fragments with similar masses in their ground states. Between these limits there is a broad region of cold heavy cluster decays. The aim of this work is to evidence cold fission valleys, which can be good candidates for the production of superheavy elements with  $Z \geq 118$ , by using the inverse, fusion process. We extend the analysis performed in Ref. [17] within a simple model, to a more reliable microscopic approach to estimate the fission/fusion barrier, given by a new version of the Super Asymmetric Two Center Shell Model [18]. This version solves a Woods-Saxon potential [19] in terms of the two center prescriptions and provides two additional degrees of freedom, that is, the deformations of the fragments. The deformation energy of the di-nuclear system is the sum between the liquid drop energy and the shells effects, including pairing corrections. The macroscopic energy is obtained within the framework of the Yukawa-plus-exponential model extended to binary systems with different charge densities [20]. Strutinsky correction prescriptions [21] were computed on the basis of a new version of the two center model with Woods-Saxon deformed potentials of fragments. We considered only cold fission/fusion process. Consequently the deformations of the initial and final nuclei are given by their ground state values of Ref. [22].

The penetrability, corresponding to some binary partition, defines the isotopic yield and it is characterized by the difference between the nuclear plus Coulomb potential and the  $Q$ -value. For a given initial nucleus ( $Z, A$ ) this quantity, called drivind potential, depends upon the charge, mass numbers

of a given fragment (we will consider the second one) and the inter-fragment distance. For a fixed combination  $A = A_1 + A_2$  the driving potential has a minimum at the charge equilibration point  $Z_2$ , which we will not mention in the following, i.e.

$$V(A_2, R) = V_N(A_2, R) + V_C(A_2, R + B(Z_1, A_1) + B(Z_2, A_2)) , \quad (1)$$

where  $V_N(A_2, R)$  is the nuclear and  $V_C(A_2, R)$  Coulomb inter-fragment potential. Here the binding energy of the initial nucleus is not considered, because it has the same value for all binary partitions. For deformed nuclei, due to the fact that the largest emission probability corresponds to the lowest barrier, this potential decreases in the direction of the largest fragment radius. We mention that a very convincing theoretical evidence that the cold fission has a sub-barrier character and depends upon deformation parameters was the calculation of penetration factors, using a double the double folding inter-fragment potential, with M3Y plus Coulomb nucleon-nucleon forces. This simple estimate was able to reproduce the gross features of the binary cold fragmentation isotopic yields from  $^{252}\text{Cf}$  [23]. Here it was shown the important role not only of quadrupole, but also of hexadecapole deformation parameters on emission probability.

Our first step is to estimate the driving potential (1) for nuclei beyond  $Z=118$ . First of all we have checked the validity of the two center shell model, by reproducing qualitatively cold isotopic yields from  $^{252}\text{Cf}$  [23]. Then, we computed the driving potential for the hypothetical compound nucleus  $^{300}_{120}\text{X}$ . This nucleus has a larger amount of neutrons than the measured superheavy combinations with  $Z=116$  and  $118$  [24]. In Fig. 1 we plotted the two dimensional potential surface  $V(A_2, R)$  versus the fragment mass number of the second partner and the inter-fragment distance  $R$ . It is clear that the cold fission/fusion process is very much hindered in the region of the large maximum between  $A_2 = 4$  and  $A_2 = 40$ .

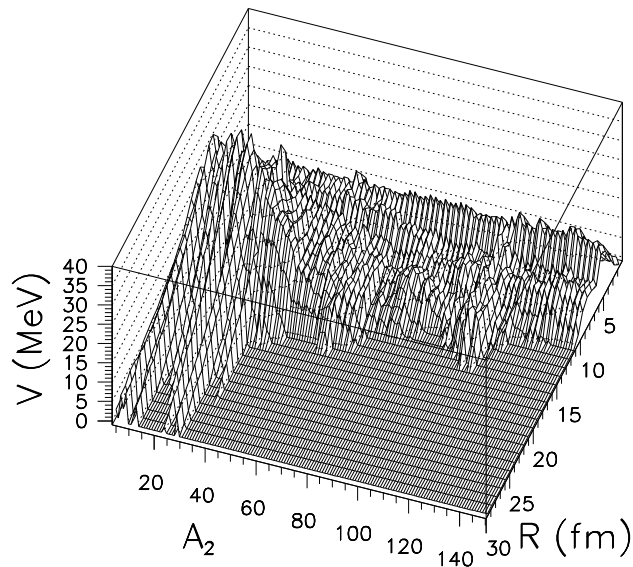


FIG. 1: The two dimensional potential  $V(A_2, R)$  versus the fragment mass number and the inter-fragment distance  $R$ , for the hypothetical compound nucleus  $^{300}_{120}\text{X}$ .

This is especially clear from Fig. 2, where we plotted the maximum value of the potential surface in Fig. 1 with respect to the inter-fragment radius  $R$ , as a function of the fragment mass number.

The first relevant minimum of the potential surface in the region  $A_2 > 40$  corresponds to the already mentioned double magic nucleus  $^{48}\text{Ca}$ , but unfortunately its binary partner  $^{252}\text{Fm}$  is unstable, as can be seen from Table 1.

In order to search for reliable binary candidates, producing the above mentioned hypothetical compound nucleus, it is necessary to investigate the penetration factor. This quantity can be estimated,

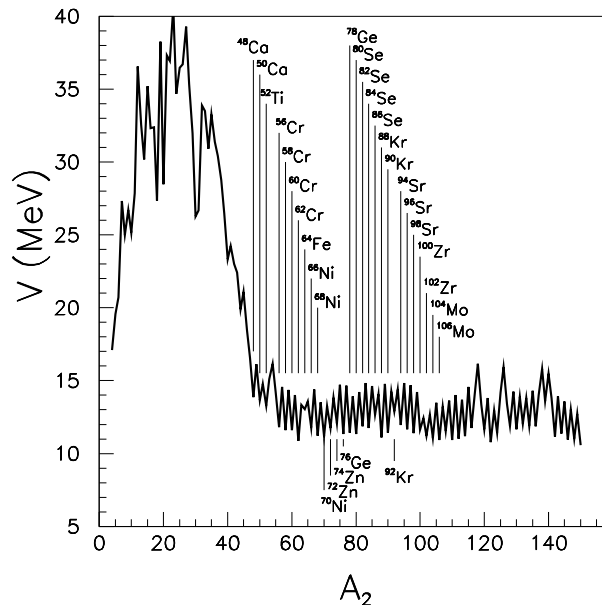


FIG. 2: The maximum value of the potential surface in Fig. 1 with respect to the inter-fragment radius  $R$ , versus the fragment mass number.

as usually, by using the semiclassical integral

$$P_{A_2} = \exp \left\{ -2 \int_{R_1}^{R_2} \sqrt{\frac{2\mu}{\hbar^2} [V(A_2, R) - B(Z, A)]} dR \right\}, \quad (2)$$

between internal and external turning points. In Fig. 3 is given the penetrability ratio  $R = P_{A_2}/P_\alpha$ , corresponding to the potential surface in Fig. 1. Several maxima, comparable or larger than the mentioned combination  $^{48}\text{Ca} + ^{252}\text{Fm}$ , are present in this figure. They correspond to Cr, Fe, Ni, Zn, Ge, Se projectiles. The most promising are the projectiles beyond Zn isotopes, where the penetrability increases by nine orders of magnitude from  $^{72}\text{Zn}$  to  $^{74}\text{Zn}$ , as can also be seen from Table 1. The region of maximal values corresponds to Sr+Pb combinations, i.e. to the already mentioned Pb valley.

On the other hand the target-projectile combinations should be relative stable. In Table 1 are given the fragment half-lives of these binary combinations, with  $A_2 > 40$ , corresponding to local maxima of the penetrability. Unfortunately the half-lives of  $^{72,74}\text{Zn}$  isotopes and their partners are fast decreasing.

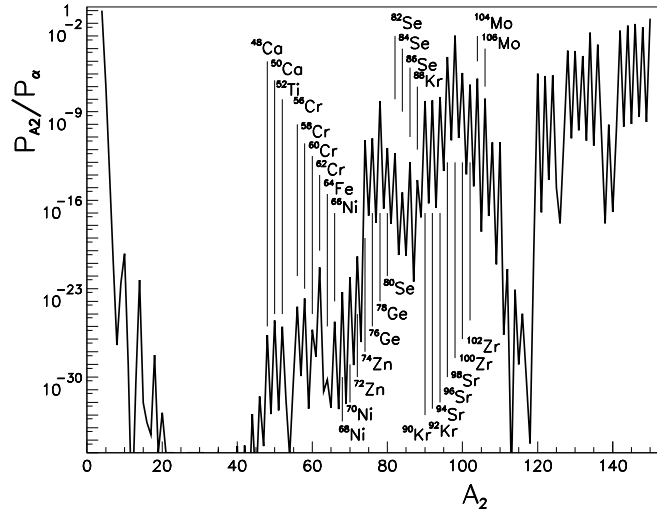


FIG. 3: The penetrabilities corresponding to the potential surface in Fig. 1 versus the mass number of the first fragment.

Table 1

Mass numbers and half-lives of binary partners for the hypothetical compound nucleus  $^{300}_{120}X$ . In the last column is given the penetrability ratio  $R = P_{A_2}/P_{\alpha}$ .

$\begin{smallmatrix} A_1 \\ Z_1 \end{smallmatrix} X_1$	$T_1$	$\begin{smallmatrix} A_2 \\ Z_2 \end{smallmatrix} X_2$	$T_2$	$R$	$\begin{smallmatrix} A_1 \\ Z_1 \end{smallmatrix} X_1$	$T_1$	$\begin{smallmatrix} A_2 \\ Z_2 \end{smallmatrix} X_2$	$T_2$	$R$
$\begin{smallmatrix} 48 \\ 20 \end{smallmatrix} \text{Ca}$	$10^{19}$ y	$\begin{smallmatrix} 252 \\ 100 \end{smallmatrix} \text{Fm}$	25.4 h	$2.1 \cdot 10^{-26}$	$\begin{smallmatrix} 76 \\ 32 \end{smallmatrix} \text{Ge}$	$10^{25}$ y	$\begin{smallmatrix} 224 \\ 88 \end{smallmatrix} \text{Ra}$	3.7 d	$8.1 \cdot 10^{-11}$
$\begin{smallmatrix} 50 \\ 20 \end{smallmatrix} \text{Ca}$	13.9 s	$\begin{smallmatrix} 250 \\ 100 \end{smallmatrix} \text{Fm}$	30 m	$3.1 \cdot 10^{-25}$	$\begin{smallmatrix} 78 \\ 32 \end{smallmatrix} \text{Ge}$	88 m	$\begin{smallmatrix} 222 \\ 88 \end{smallmatrix} \text{Ra}$	38.0 s	$7.1 \cdot 10^{-08}$
$\begin{smallmatrix} 52 \\ 22 \end{smallmatrix} \text{Ti}$	1.7 s	$\begin{smallmatrix} 248 \\ 98 \end{smallmatrix} \text{Cf}$	333.5 d	$9.5 \cdot 10^{-26}$	$\begin{smallmatrix} 80 \\ 34 \end{smallmatrix} \text{Se}$	stable	$\begin{smallmatrix} 220 \\ 86 \end{smallmatrix} \text{Rn}$	55.6 s	$1.4 \cdot 10^{-11}$
$\begin{smallmatrix} 56 \\ 24 \end{smallmatrix} \text{Cr}$	5.94 m	$\begin{smallmatrix} 244 \\ 96 \end{smallmatrix} \text{Cm}$	18.1 y	$3.7 \cdot 10^{-24}$	$\begin{smallmatrix} 82 \\ 34 \end{smallmatrix} \text{Se}$	$10^{19}$ y	$\begin{smallmatrix} 218 \\ 86 \end{smallmatrix} \text{Rn}$	35 ms	$5.2 \cdot 10^{-12}$
$\begin{smallmatrix} 58 \\ 24 \end{smallmatrix} \text{Cr}$	7 s	$\begin{smallmatrix} 242 \\ 96 \end{smallmatrix} \text{Cm}$	162.8 d	$1.7 \cdot 10^{-23}$	$\begin{smallmatrix} 84 \\ 34 \end{smallmatrix} \text{Se}$	3.1 m	$\begin{smallmatrix} 216 \\ 86 \end{smallmatrix} \text{Rn}$	45 $\mu\text{s}$	$4.1 \cdot 10^{-15}$
$\begin{smallmatrix} 60 \\ 24 \end{smallmatrix} \text{Cr}$	490 ms	$\begin{smallmatrix} 240 \\ 96 \end{smallmatrix} \text{Cm}$	27 d	$5.5 \cdot 10^{-26}$	$\begin{smallmatrix} 86 \\ 34 \end{smallmatrix} \text{Se}$	15.3 s	$\begin{smallmatrix} 214 \\ 86 \end{smallmatrix} \text{Rn}$	270 ns	$1.0 \cdot 10^{-12}$
$\begin{smallmatrix} 62 \\ 24 \end{smallmatrix} \text{Cr}$	160 ms	$\begin{smallmatrix} 238 \\ 96 \end{smallmatrix} \text{Cm}$	2.4 h	$4.8 \cdot 10^{-21}$	$\begin{smallmatrix} 88 \\ 36 \end{smallmatrix} \text{Kr}$	2.84 h	$\begin{smallmatrix} 212 \\ 84 \end{smallmatrix} \text{Po}$	299 ns	$3.9 \cdot 10^{-14}$
$\begin{smallmatrix} 64 \\ 26 \end{smallmatrix} \text{Fe}$	2 s	$\begin{smallmatrix} 236 \\ 94 \end{smallmatrix} \text{Pu}$	2.9 y	$6.3 \cdot 10^{-30}$	$\begin{smallmatrix} 90 \\ 36 \end{smallmatrix} \text{Kr}$	32.3 s	$\begin{smallmatrix} 210 \\ 84 \end{smallmatrix} \text{Po}$	138.4 d	$7.4 \cdot 10^{-08}$
$\begin{smallmatrix} 66 \\ 28 \end{smallmatrix} \text{Ni}$	54 h	$\begin{smallmatrix} 234 \\ 92 \end{smallmatrix} \text{U}$	$2.5 \cdot 10^5$ y	$2.5 \cdot 10^{-25}$	$\begin{smallmatrix} 92 \\ 36 \end{smallmatrix} \text{Kr}$	1.84 s	$\begin{smallmatrix} 208 \\ 84 \end{smallmatrix} \text{Po}$	2.9 y	$8.1 \cdot 10^{-08}$
$\begin{smallmatrix} 68 \\ 28 \end{smallmatrix} \text{Ni}$	29 s	$\begin{smallmatrix} 232 \\ 92 \end{smallmatrix} \text{U}$	68.9 y	$5.4 \cdot 10^{-23}$	$\begin{smallmatrix} 94 \\ 38 \end{smallmatrix} \text{Sr}$	75.3 s	$\begin{smallmatrix} 206 \\ 82 \end{smallmatrix} \text{Pb}$	stable	$1.4 \cdot 10^{-07}$
$\begin{smallmatrix} 70 \\ 28 \end{smallmatrix} \text{Ni}$	1 $\mu\text{s}$	$\begin{smallmatrix} 230 \\ 92 \end{smallmatrix} \text{U}$	20.8 d	$8.1 \cdot 10^{-22}$	$\begin{smallmatrix} 96 \\ 38 \end{smallmatrix} \text{Sr}$	1 s	$\begin{smallmatrix} 204 \\ 82 \end{smallmatrix} \text{Pb}$	stable	$2.2 \cdot 10^{-04}$
$\begin{smallmatrix} 72 \\ 30 \end{smallmatrix} \text{Zn}$	46.5 h	$\begin{smallmatrix} 228 \\ 90 \end{smallmatrix} \text{Th}$	1.9 y	$3.7 \cdot 10^{-20}$	$\begin{smallmatrix} 98 \\ 38 \end{smallmatrix} \text{Sr}$	653 ms	$\begin{smallmatrix} 202 \\ 82 \end{smallmatrix} \text{Pb}$	$5.2 \cdot 10^3$ y	$1.1 \cdot 10^{-02}$
$\begin{smallmatrix} 74 \\ 30 \end{smallmatrix} \text{Zn}$	95.6 s	$\begin{smallmatrix} 226 \\ 90 \end{smallmatrix} \text{Th}$	30.6 m	$5.7 \cdot 10^{-11}$					

In order to compare the data in Table 1 with those corresponding to some experimentally detected superheavy elements, in Table 2 we give penetrability ratios of three measured fusion reactions.

We also compared the penetrabilities in Table 1 with the corresponding quantities of some close elements which have been experimentally reported by using  $^{48}\text{Ca}$  as projectile. The reactions given in the first and second lines of the Table 2 have penetrability ratios around  $R \approx 10^{-24}$ . The corresponding values of the first two lines in Table 1 are not far from this number.

Table 2

Mass numbers and half-lives of binary partners for the experimentally detected compound nuclei  $^A_Z X$ . In the last columns is given the penetrability ratio  $R = P_{A_2}/P_{\alpha}$  and the quoted reference.

$\begin{smallmatrix} A_1 \\ Z_1 \end{smallmatrix} X_1$	$T_1$	$\begin{smallmatrix} A_2 \\ Z_2 \end{smallmatrix} X_2$	$T_2$	$\begin{smallmatrix} A \\ Z \end{smallmatrix} X$	$R$	Ref.
$\begin{smallmatrix} 48 \\ 20 \end{smallmatrix} \text{Ca}$	$10^{19}$ y	$\begin{smallmatrix} 244 \\ 96 \end{smallmatrix} \text{Cm}$	18.1 y	$\begin{smallmatrix} 292 \\ 116 \end{smallmatrix} \text{X}$	$1.7 \cdot 10^{-24}$	[24]
$\begin{smallmatrix} 48 \\ 20 \end{smallmatrix} \text{Ca}$	$10^{19}$ y	$\begin{smallmatrix} 246 \\ 98 \end{smallmatrix} \text{Cf}$	35.7 h	$\begin{smallmatrix} 294 \\ 118 \end{smallmatrix} \text{X}$	$1.1 \cdot 10^{-24}$	[24]
$\begin{smallmatrix} 70 \\ 30 \end{smallmatrix} \text{Zn}$	stable	$\begin{smallmatrix} 208 \\ 82 \end{smallmatrix} \text{Pb}$	stable	$\begin{smallmatrix} 278 \\ 112 \end{smallmatrix} \text{X}$	$5.0 \cdot 10^{-11}$	[25]

The penetrability ratio, corresponding to the third reaction  $^{208}\text{Pb} + ^{70}\text{Zn} \rightarrow ^{278}_{112}\text{X}$  [25], is  $R = P_{A_2}/P_\alpha \approx 5 \cdot 10^{-11}$ . Practically all combination beyond  $^{74}\text{Zn}$ , giving the hypothetical element  $^{300}_{120}\text{X}$ , have the penetrability ratios larger than this value. In Table 1 we remark that in the combination  $^{76}\text{Ge} + ^{224}\text{Ra}$  both partners have enough large half-lives to be used in fusion experiments.

Concluding, we computed the potential energy surface for different binary combinations, giving the superheavy compound nucleus  $^{300}_{120}\text{X}$ , by using the Two Center Shell Model. We evidenced binary partners whose penetration factors are comparable with similar combinations, producing close superheavy elements which were experimentally measured. An extensive analysis on fission/fusion channels for all possible isotopes in this region of superheavy elements, by using this performant version of the Two Center Shell Model, is under way.

- 
- [1] G.N. Flerov, *Atom. Ener.* **26**, 138 (1969).
  - [2] A. Săndulescu, R.K. Gupta, W. Scheid, and W. Greiner, *Phys. Lett.* **60** B, 225 (1976).
  - [3] R.K. Gupta, C. Parvulescu, A. Săndulescu, and W. Greiner, *Z. Phys. A* **283**, 217 (1977).
  - [4] R.K. Gupta, A. Săndulescu, and W. Greiner, *Phys. Lett. bf* **67** B, 257 (1977).
  - [5] A. Săndulescu, D. Poenaru, and W. Greiner, *Fiz. Elem. Chastits At. Yadra* **11**, 1334; *Sov. J. Part. Nucl.* **11**, 528 (1980).
  - [6] Yu. Ts. Oganessian, *Nucl. Phys. A* **685**, 17c (2001).
  - [7] Yu. Ts. Oganessian, *et. al.* *Nucl. Phys. A* **734**, 109 (2004).
  - [8] S. Hofmann and G. Münzenberg, *Rev. Mod. Phys.* **72**, 733 (2000).
  - [9] S. Hofmann, G. Münzenberg, and M. Schädel, *Nucl. Phys. News* **14** No. 4, 5 (2004).
  - [10] V. Yu. Denisov and S. Hofmann, *Phys. Rev. C* **61**, 034606 (2000).
  - [11] R. Smolanczuk, *Phys. Rev. C* **63**, 044607 (2001).
  - [12] V.I. Zagrebaev, Y. Arimoto, M.G. Itkis, and Yu. Ts. Oganessian, *Phys. Rev. C* **65**, 014607 (2001).
  - [13] M.G. Itkis, Yu. Ts. Oganessioan, and V.I. Zagrebaev, *Phys. Rev. C* **65**, 044602 (2002).
  - [14] Y.K. Gambhir, A. Bhagwat, and M. Gupta, *Phys. Rev. C* **71**, 037301 (2005).
  - [15] G. Gamow *Z. Phys.* **51**, 204 (1928).
  - [16] D.S. Delion, A. Săndulescu, and W. Greiner, *Phys. Rev. C* **69**, 044318 (2004).
  - [17] D.S. Delion and A. Săndulescu, *Rom. J. Phys.* **52**, 43 (2007).
  - [18] M. Mirea, *Phys. Rev. C* **57**, 2484 (1998).
  - [19] M. Mirea, *Rom. Rep. Phys.* **59**, 523 (2007).
  - [20] D.N. Poenaru, M. Ivascu and D. Mazilu, *Comput. Phys. Commun.* **19**, 205 (1980).
  - [21] M. Brack, J. Damgaard, A. Jensen, H. Pauli, V. Strutinsky and W. Wong, *Rev. Mod. Phys.* **44**, **320** (1972).
  - [22] P. Möller, J.R. Nix, W.D. Myers, and W.J. Swyatecki, *At. Data Nucl. Data Tables* **59**, 185 (1995).
  - [23] A. Săndulescu, Ș. Mișicu, F. Carstoiu, A. Florescu, and W. Greiner, *Phys. Rev. C* **57**, 2321 (1998).
  - [24] Yu. Ts. Oganessian, *et.al.*, JINR Preprint E7-2004-160.
  - [25] S. Hofmann, *et.al.*, *Z. Phys. A* **354**, 229 (1996).